Pergamon

PII: S0301-9322(96)00020-1

Int. J. Multiphase Flow Vol. 22, No. 5, pp. 893–908, 1996

0301-9322/96 $15.00 + 0.00

CONDENSATION OF PURE STEAM AND STEAM–AIR MIXTURE WITH SURFACE WAVES OF CONDENSATE FILM ON A VERTICAL WALL

S. K. PARK[1], M. H. KIM and K. J. YOO[2]

[1]Department of Mechanical Engineering, POSTECH San 31, Hyoja-dong, Pohang, 790-784, Korea
[2]Korea Atomic Energy Research Institute, Daeduck Danji, P.O. Box 7, Taejon, Korea

(Received 30 September 1995; in revised form 7 April 1996)

Abstract—A series of experiments has been conducted to investigate the effect of wavy interface on film condensation with and without a noncondensable gas present on a vertical wall. Concurrently, the instantaneous film thickness was measured. Overall heat transfer coefficients across the condensate film and the diffusion layer formed by a noncondensable gas were obtained in various parameters such as air–mass fraction ($W = 0.1$–0.7), mixture vapor velocity ($U_{in} = 3, 5, 7$ m/s) and condensate film Reynolds number ($Re_{f,in} = 0$–$19{,}000$). In order to investigate the heat transfer enhancement induced by a dynamic interaction of the surface waves on condensate and the diffusion layer, vapor-side heat transfer coefficient was estimated from the measured overall heat transfer coefficient and the correlation of film-side heat transfer coefficient, and compared with that estimated by Colburn and Chilton–Colburn analogy for a smooth flat plate. The comparison showed that the vapor-side heat transfer coefficient increased clearly with the increase of film Reynolds number. The enhancement effect was dominant for low mixture vapor velocity and decreased with the increase of mixture vapor velocity. Copyright © 1996 Elsevier Science Ltd.

Key Words: condensation, noncondensable gas, steam, air, wave, condensate film

1. INTRODUCTION

After Othmer (1929) showed in his steam–air condensation experiment that heat transfer can be reduced significantly due to a small amount of noncondensable gas, a great number of studies on the effect of a noncondensable gas have been conducted both theoretically and experimentally. The theoretical studies were conducted on the limited flow regime, laminar condensate film and laminar mixture vapor flow (Minkowycz & Sparrow 1966; Sparrow *et al.* 1967; Denny *et al.* 1971; Denny & Jusionis 1972). It was assumed, in these works, that the interface between condensate film and mixture vapor was smooth without waves.

Most of the experimental results, overall heat transfer coefficient across the condensate film and the diffusion layer of mixture vapor phase, were correlated in terms of a reduction factor to the pure steam condensation as a function of noncondensable gas concentration (Henderson & Marchello 1969; Sleger & Seban 1970; Al-Diwany & Rose 1973; Asano & Nakano 1978). In recent, Peterson *et al.* (1993) derived an effective "condensation" thermal conductivity from an appropriate thermodynamic relationship and the fundamental solution for mass transport in diffusion layers with noncondensables. With the formulation and the experimental result for a vertical tube, they determined that vapor condensation obeyed the analogy between heat and mass transfer.

Dallmeyer (1970) studied experimentally the turbulent boundary layers of velocity, temperature and concentration, when the mixture vapor of air and CCl_4 condensed on a vertical flat surface. Legay-Desesquelles & Prunet-Foch (1986) also investigated experimentally the turbulent boundary layers in the steam–air condensation. However, these research removed the condensate film in order to maintain laminar flow and smooth interface everywhere. The effects of surface waves on the condensation heat transfer of mixture vapor were not investigated.

Stability analyses and experimental observation on falling-film on a vertical wall have shown that various surface waves according to film Reynolds number appeared due to the intrinsic instabilities (Chu & Dukler 1974; Spindler 1982; Kang & Kim 1992; Chang 1994). These waves were known

as a mechanism to enhance heat and mass transfer in the film (Chun & Seban 1971; Kutateladze & Gogonin 1979; Kellenbenz & Hahane 1994). Also, these waves are expected to enhance the transport of heat and mass in the vapor phase as well as the liquid phase. Since the noncondensable gas at very near the interface are a principal source of thermal resistance, a disturbance of the interface might enhance heat and mass transfer considerably for the mixture vapor condensation in the presence of noncondensable gas.

However, much less attention has been paid to the effect of surface waves on heat and mass transfer in the diffusion layer. This effect was considered by Kim & Corradini (1990) recently. In their model, the wavy interface was treated as a hydrodynamic rough surface. Afterwards Kang & Kim (1994) conducted an experiment of steam–air condensation in a nearly horizontal (4.1°) square duct to investigate the effect of surface waves. Karapantsios *et al.* (1995), in their experiments of steam–air condensation, showed that the dependence of heat transfer coefficients on the liquid flow rate was attributed to the dynamic interaction between the interfacial waves and the mixture vapor layer. In these experiments the steam–air mixture condensed into liquid in direct contact with subcooled water layers inside a vertical tube. The mixture vapor was maintained effectively stagnant. Huhtiniemi & Corradini (1993) studied experimentally the orientation effect of condensing surface on steam–air condensation. By tilting the condensing surface from the horizontal to the vertical position, the heat transfer coefficient changed 15–25% depending on the air–mass fraction. The dependency of the heat transfer coefficient on the orientation was caused by the flow characteristics and the surface structure of condensate film.

Inspite of some experimental studies, the knowledge of surface wave effects on heat and mass transfer is insufficient, especially, for the condensation of mixture vapor with a noncondensable gas. To investigate the effect of surface waves of condensate film on pure vapor and mixture vapor condensation, a series of experiments has been conducted in a nearly vertical rectangular duct (87.5° to horizontal plane). The parameters considered were air–mass fraction ($W = 0.1$–0.7; defined as mass flow rate of air over mass flow rate of steam–air mixture), mixture vapor velocity ($U_m = 3$, 5, 7 m/s; based on the inlet of the test section), and condensate film Reynolds number ($Re_{f,in} = 0$–$19{,}000$; based on the inlet of the test section). To investigate the various surface waves in a broad range of film Reynolds number, extra condensate film was fed. All experiments were conducted at atmospheric pressure.

Main result is overall heat transfer coefficient across the condensate film and the diffusion layer formed by a noncondensable gas. Especially, vapor-side heat transfer coefficient was reduced from the overall heat transfer coefficient and the film-side heat transfer coefficient. By considering the present experimental results of vapor-side heat transfer coefficient and the estimation of that by Colburn and Chilton–Colburn analogy for a flat plate, the effect of surface waves on heat and mass transfer in the diffusion layer was investigated. Also, the characteristics of the surface waves was presented and discussed.

2. EXPERIMENTS

2.1. *Experimental facilities*

The experimental facilities consisted of the test section and the auxiliary equipment; the mixture vapor supplying unit, the condensate film supplying loop to control film Reynolds number and the cooling water loop to remove the latent heat.

Mixture vapor was provided by a steam generator operated at 686 kPa gauge pressure and an air blower. When low mass flow rate was needed, compressed air was used. The steam was regulated to 19.0–49.0 kPa and mixed with the heated air. The steam flow rate was measured by an orifice flow meter and automatically adjusted to a desired value by the feedback control valve. Also, the air flow rate was measured by an orifice flow meter. The orifice flow meters were constructed according to ASME specifications (1971). The rotary meter (FL400A-OMEGA) was specifically used for the flow rate below 0.01 m^3/s. The accuracy was guaranteed within $\pm 2\%$.

The description of the test section is shown in figure 1. The mixture vapor and the fed film flowed down concurrently through the rectangular duct. The width and the height of the duct were 150 and 100 mm, respectively. The length of the duct and the condensing wall were 1750 and 1510 mm

long, respectively. The length of the cooling surface and the cross-sectional size of the test duct were designed so that the boundary layers at the opposite walls did not interact. A settling chamber to enhance the quality of mixture vapor flow was located in front of the test section. The temperatures of the mixture vapor were measured at the inlet and the outlet of the duct.

The condensate film was circulated through the insulated closed loop and the flow rate was measured by the magnetic flow meter. The stationary condensate was supplied from the constant head tank located above the test section inlet. The temperatures of the liquid were measured at the inlet and the outlet to confirm whether they were equivalent to the saturate liquid temperature or not. Coolant water was circulated through the closed loop to remove the condensation heat. The coolant temperature was controlled to maintain the optimum difference of temperature between the mixture vapor and the condensing wall. In all measurements, the wall temperature was maintained constant within $\pm 0.1°C$ of a given condition. The coolant water was sufficiently supplied, so the increase of the coolant temperature ($T_{f,out}$) at outlet was less than 1.5°C even at the time of maximum heat flux.

All temperatures were measured by calibrated T-type thermocouples and Keithley DAS (Data Acquisition System). With linked to the each channel of the DAS, each thermocouples was calibrated by a platinum resistance thermometer at constant water bath from 20 to 100°C.

2.2. *Measurement of heat flux*

Figure 2 shows the side and the cross-sectional views of the cooling block. The size of the cooling block was 1510 mm long, 150 mm wide and 24 mm thick. Thirty eight T-type thermocouples were installed at 2 mm inward from the upper and the lower sides to measure local heat flux. The other sides were carefully insulated to make adiabatic condition.

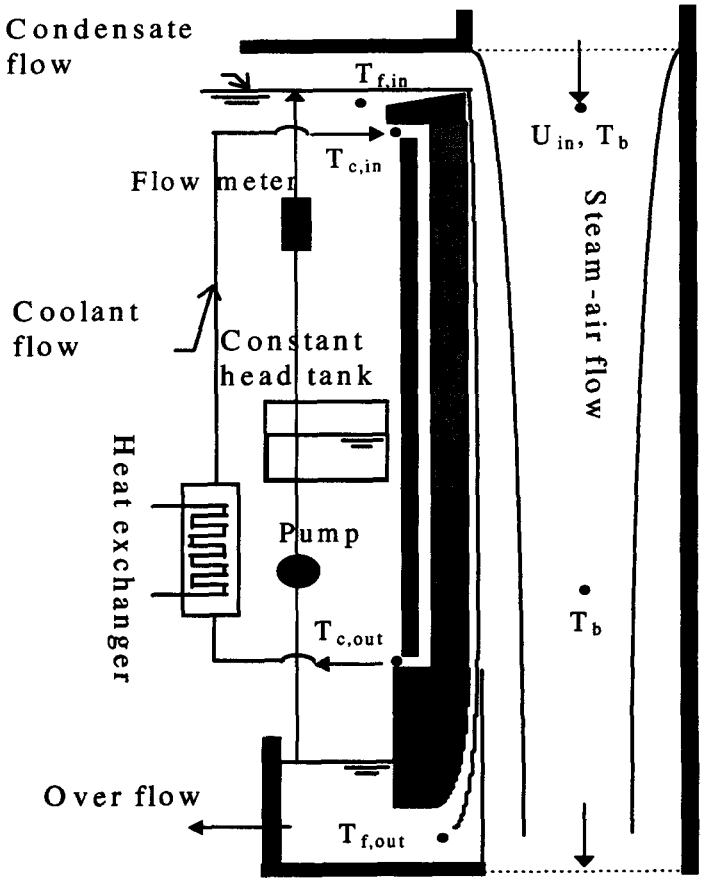

Figure 1. Side view of test section.

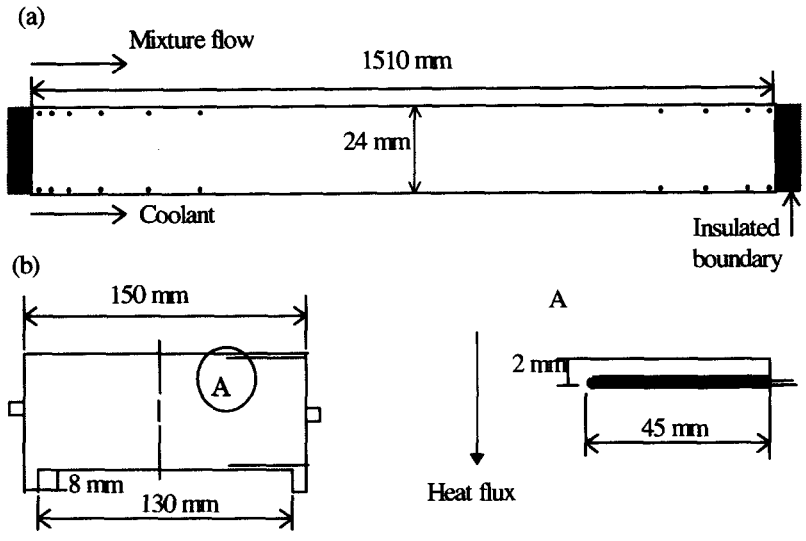

Figure 2. Configuration of thermocouple sensors installed in the cooling block. (a) Side view; (b) cross sectional view.

The local heat flux was calculated from the 2-dimensional conduction equation and the proper boundary conditions which were the temperatures measured at the upper and the lower sides of the block and the adiabatic condition at the other sides. The cooling block was aluminum alloy in which thermal conductivity was precisely measured with the Ulyac TC-7000 HNC thermal conductivity meter. It was 127 W/mK.

This method was checked by the direct measurement of condensate in pure steam condensation without the fed film. The condensate was measured at the end of the condensing wall and compared with the calculated one from the measured heat flux and the latent heat. The direct measurement

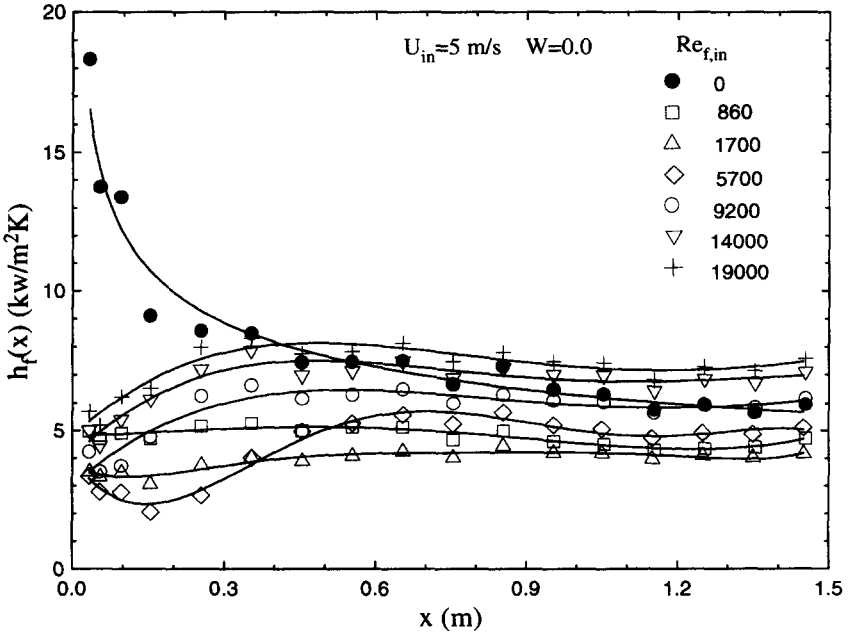

Figure 3. Heat transfer coefficients along the condensing wall with and without feed water in pure steam condensation.

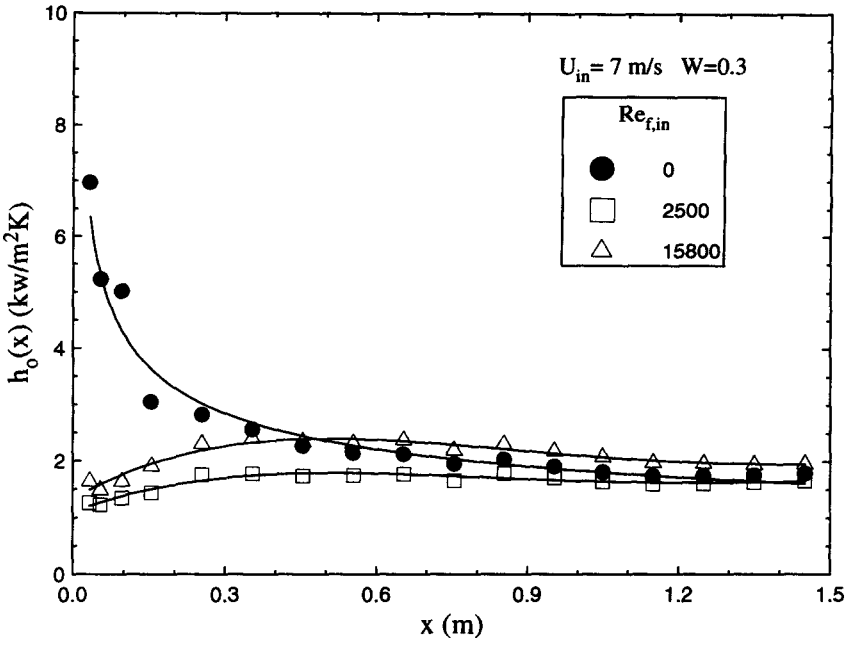

Figure 4. Heat transfer coefficients along the condensing wall with and without feed water in steam–air condensation.

was greater 4.3% than the calculated one. The repeatability of the direct measurement is within ±2%.

2.3. *Measurement of condensate film thickness*

Surface waves of condensate were measured by flush-wire probe developed by Kang & Kim (1992). Double wire electrodes of 0.075 mm diameter and aluminum block were used as the measuring electrode and the source electrode respectively. All data, 62,000 points per probe, were recorded at 5 kHz. The probe was mounted on the upper plate of the test duct and moved to a 0.01 mm resolution by micrometer. The whole process of measurement was observed from the window of the test section.

Instantaneous film thickness was obtained simultaneously at two locations of 1.3 m away from the top of the condensing wall. The measuring electrodes were separately located by 29.0 mm along the stream-wise direction in order to measure the celerity. The calibration curve between voltage signal and film thickness was obtained through the method developed by Kang & Kim (1992), which was based on probability of liquid's existence at a given height. Since the calibration does not directly depend on the electrical properties of liquid, it is very useful to measure condensate film thickness.

Table 1. Experimental conditions

U_{in} (m/s)	$Re_{f,in}$	W	$T_{b,s}$ (°C)†	T_w (°C)‡	U_{in} (m/s)	$Re_{f,in}$	W	$T_{b,s}$ (°C)†	T_w (°C)‡
3	0–19,000	0.0	100.	89.2	5	0–18,000	0.1	98.1	84.1
3	0–13,000	0.1	98.1	78.2	5	0–16,000	0.2	95.9	76.8
3	0–16,000	0.2	95.9	78.5	5	0–16,000	0.3	93.4	75.1
3	0–14,000	0.3	93.4	66.4	5	0–13,000	0.5	86.9	60.6
3	0–15,000	0.3	93.4	75.2	5	0–14,000	0.5	86.9	69.5
3	0–12,000	0.5	86.9	58.7	5	0–12,000	0.7	76.6	58.6
3	0–14,000	0.5	86.9	68.6	6	0–18,000	0.0	100.	90.8
3	0–12,000	0.7	76.6	58.0	7	0–17,000	0.2	95.9	81.1
3	0–14,000	0.7	76.6	49.5	7	0–16,000	0.3	93.4	76.0
5	0–19,000	0.0	100.	90.3	7	0–14,000	0.5	86.9	68.2

†Saturation temperature of steam–air mixture in the core of test section.
‡Mean temperature of condensing wall.

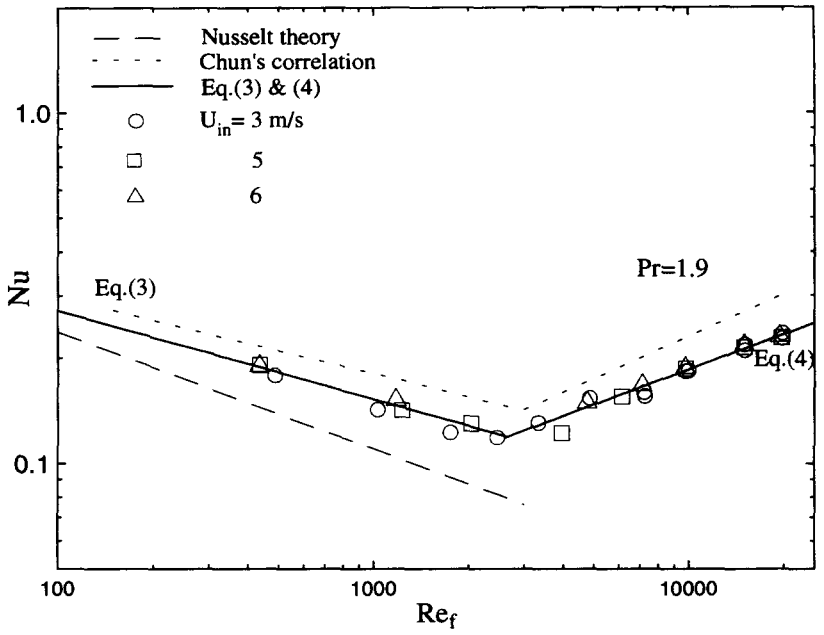

Figure 5. Comparison of local Nusselt number with the previous work.

2.4. *Reduction of experimental results*

Local heat transfer coefficients for mixture vapor condensation are defined as following equation,

$$q(x) = h_o(T_{b,s} - T_w) = h_f(T_i - T_w) = h_v(T_{b,s} - T_i) \quad [1]$$

where h_o, h_f and h_v are overall, film-side and vapor-side heat transfer coefficient, respectively. $T_{b,s}$ and T_i, are the saturated temperature of mixture vapor and interface between the two phases. The temperature difference between $T_{b,s}$ and T_i is caused the existence of air (noncondensable gas). For

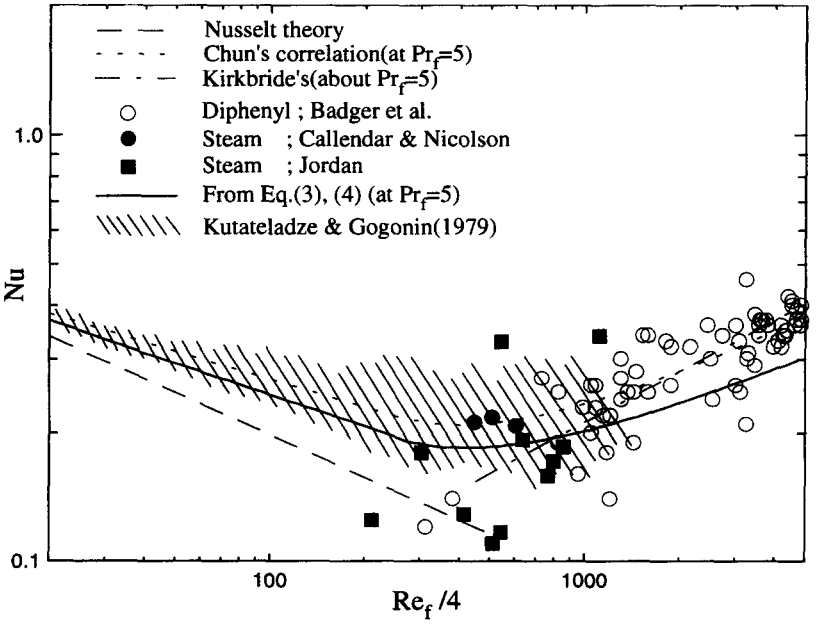

Figure 6. Comparison of mean Nusselt number with the previous work (from Kirkbride 1933–1934).

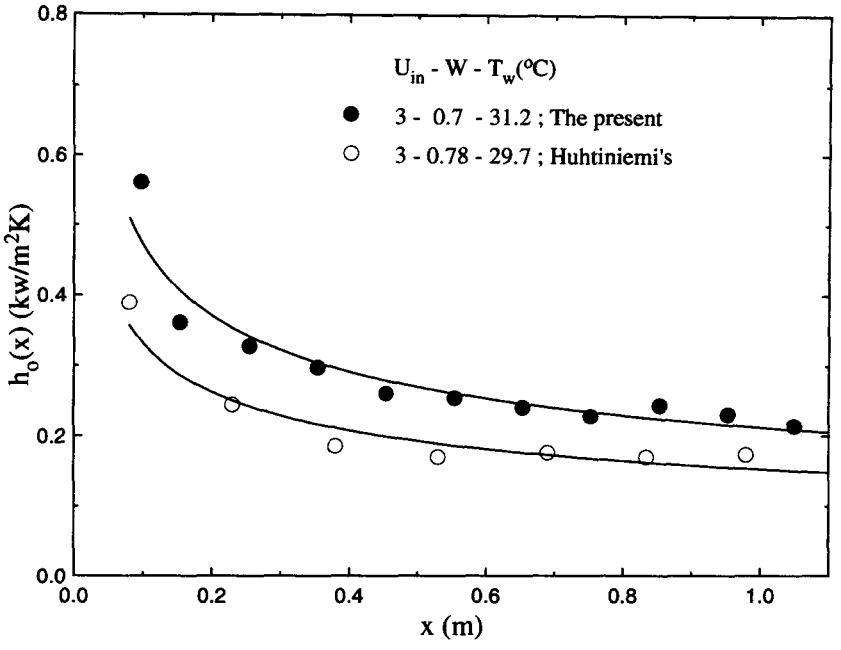

Figure 7. Comparison of heat transfer coefficients without feed water.

mixture vapor condensation, steam concentration decreases and air concentration increases at near the condensate film. The temperature of the interface is low than that of bulk vapor. T_w is the surface temperature of condensing wall. The surface temperature was calculated from the temperature measured at 2 mm below wall surface of the cooling block by using the heat flux measured. Overall heat transfer coefficient, h_o, was primitive value calculated from the measured $T_{b,s}$, T_w, and $q(x)$. Interface temperature, T_i, was estimated to analyze the vapor-side heat transfer coefficient. The detail method is to be explained in the following section. In the case of saturated

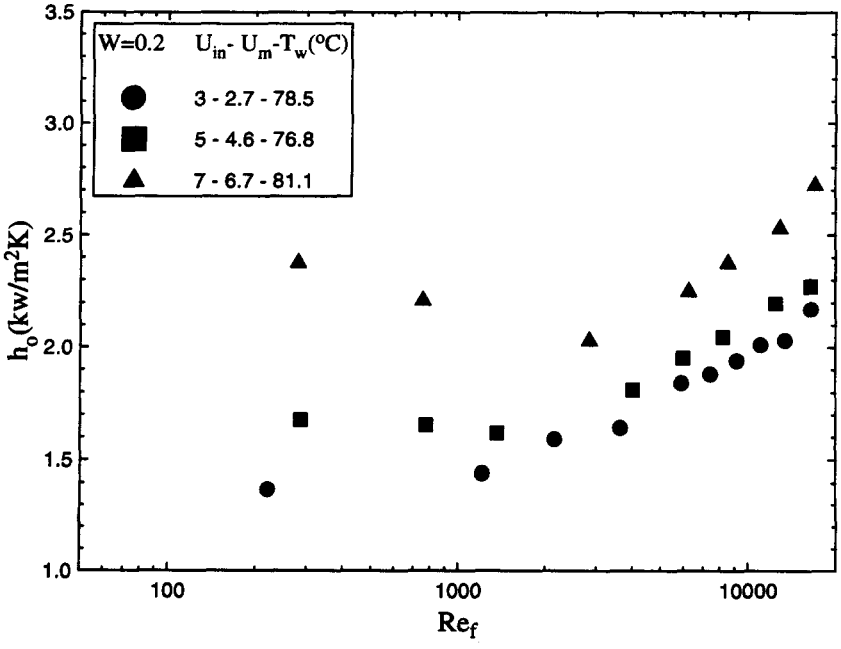

Figure 8. Overall heat transfer coefficients with condensate film Reynolds number ($T_{b,s}$ = 95.9°C).

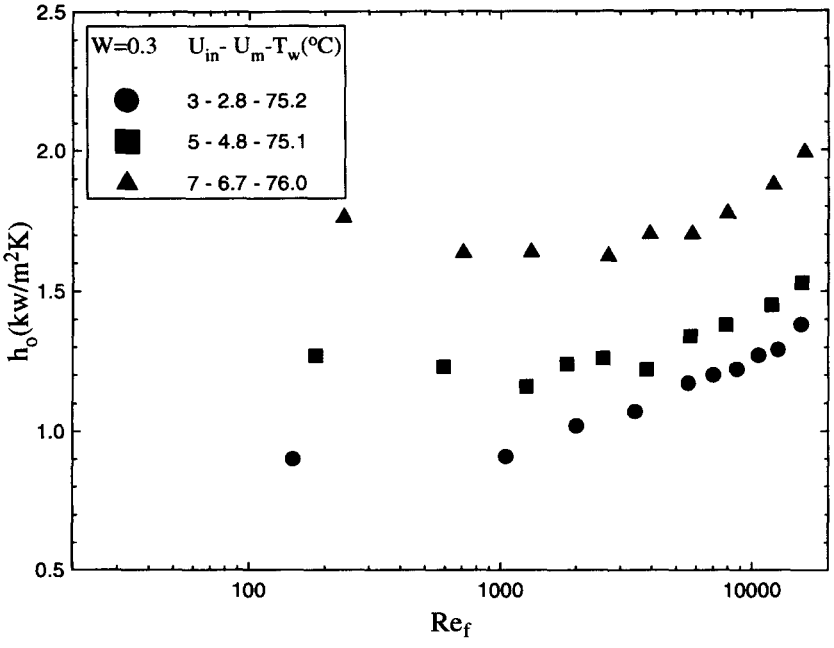

Figure 9. Overall heat transfer coefficients with condensate film Reynolds number ($T_{b,s}$ = 93.4°C).

pure steam condensation, $T_{b,s}$, and T_i are same. So, h_o and h_f are equivalent, and h_v can not be defined.

Figures 3 and 4 show the typical results of the local overall heat transfer coefficient along the condensing surface with and without the fed film. The result for the non-feeding cases ($Re_{f,in} = 0$) shows a trend similar to Nusselt theory (1916), whereas the results for the feeding cases ($Re_{f,in} > 0$) show transition region at near the entrance of the test section. This is because the thermal and hydrodynamic conditions of the liquid film are not completely equivalent to those of natural

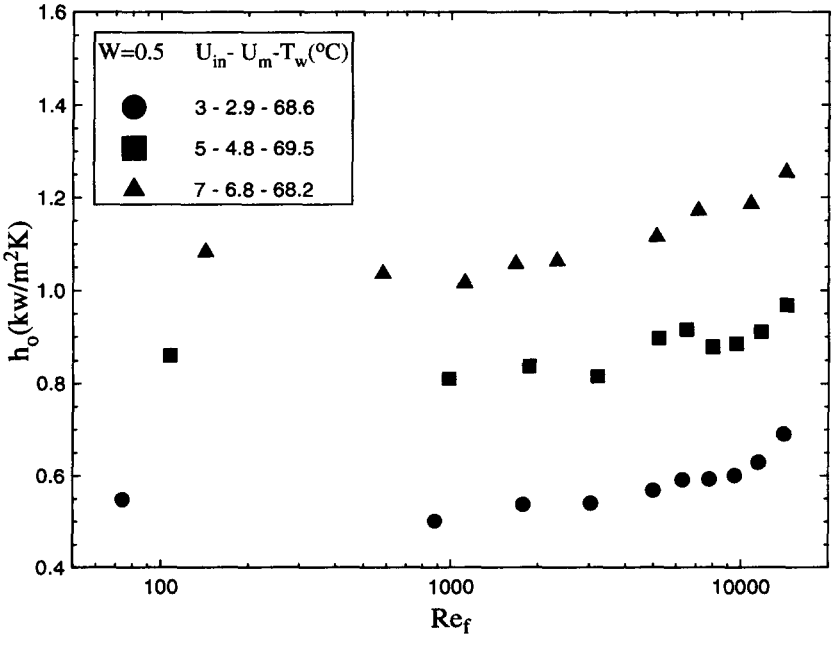

Figure 10. Overall heat transfer coefficients with condensate film Reynolds number ($T_{b,s}$ = 86.9°C).

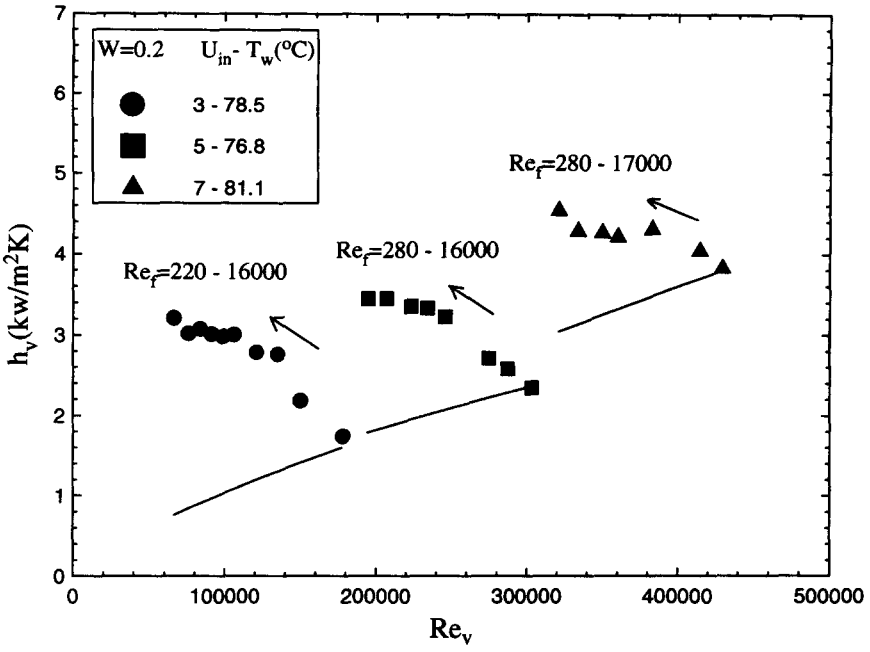

Figure 11. Vapor-side heat transfer coefficients ($T_{b,s}$ = 95.9°C).

condensate. As the fed film develops thermally and hydrodynamically, however, the local heat transfer coefficients show an inherent characteristics similar to the non-feeding cases. So, when the extra condensate was fed, only the heat transfer coefficient in the interval (x = 1.1–1.5 m) was taken for the heat transfer analyses. Figures 3 and 4 also show that the change of heat transfer coefficient after about 1.1 m from the entrance is negligible regardless of the film feeding. This was satisfied in all the experiments listed in table 1. Therefore, the localized mean of the interval (x = 1.1–1.5 m) was analyzed as local heat transfer coefficient at the x = 1.3 m.

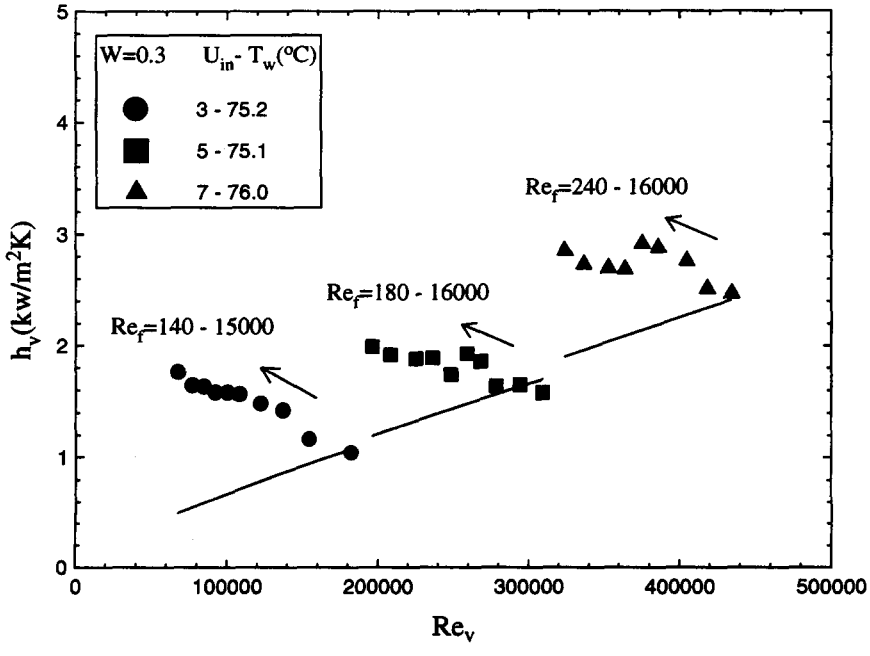

Figure 12. Vapor-side heat transfer coefficients ($T_{b,s}$ = 93.4°C).

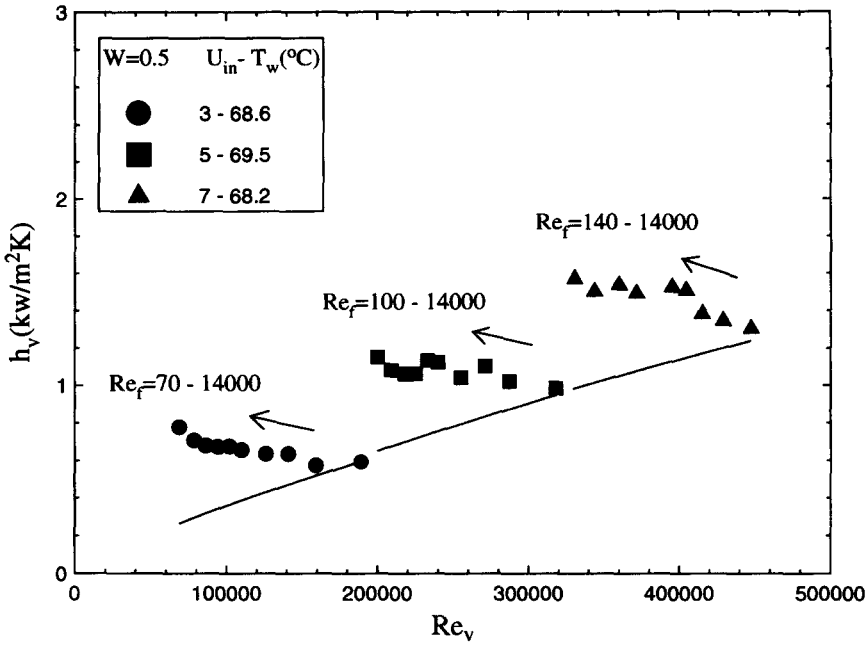

Figure 13. Vapor-side heat transfer coefficients ($T_{b,s}$ = 86.9°C).

Local film Reynolds number was calculated from the fed film flow rate and the condensate as in the following equation,

$$\mathrm{Re}_f = \frac{4}{\mu} m'(x) = \frac{4}{\mu} m'_{in}\left[1 + \frac{1}{m'_{in} i_{fv} x}\int_0^x q(x')\mathrm{d}x'\right] \qquad [2]$$

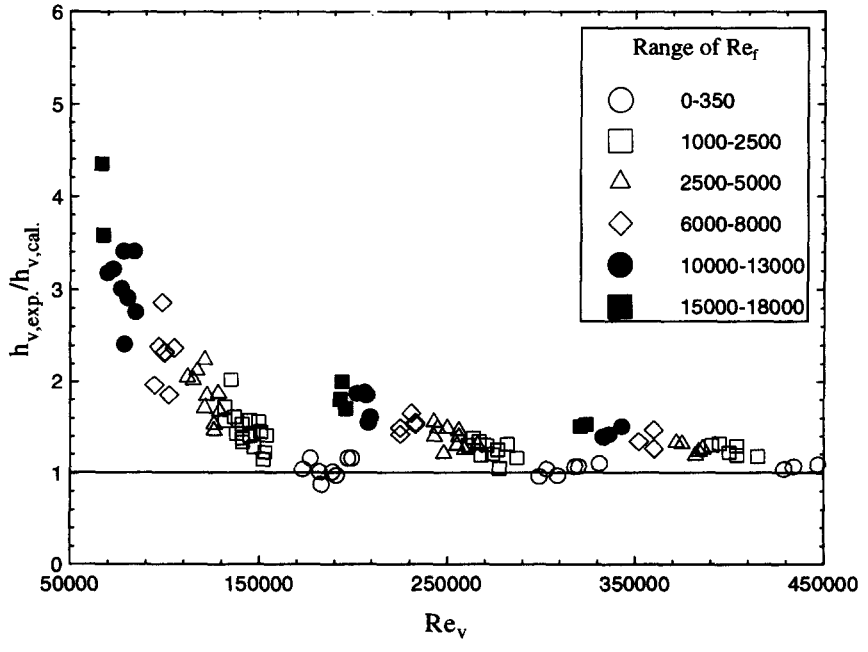

Figure 14. Enhancement effect of vapor-side heat transfer.

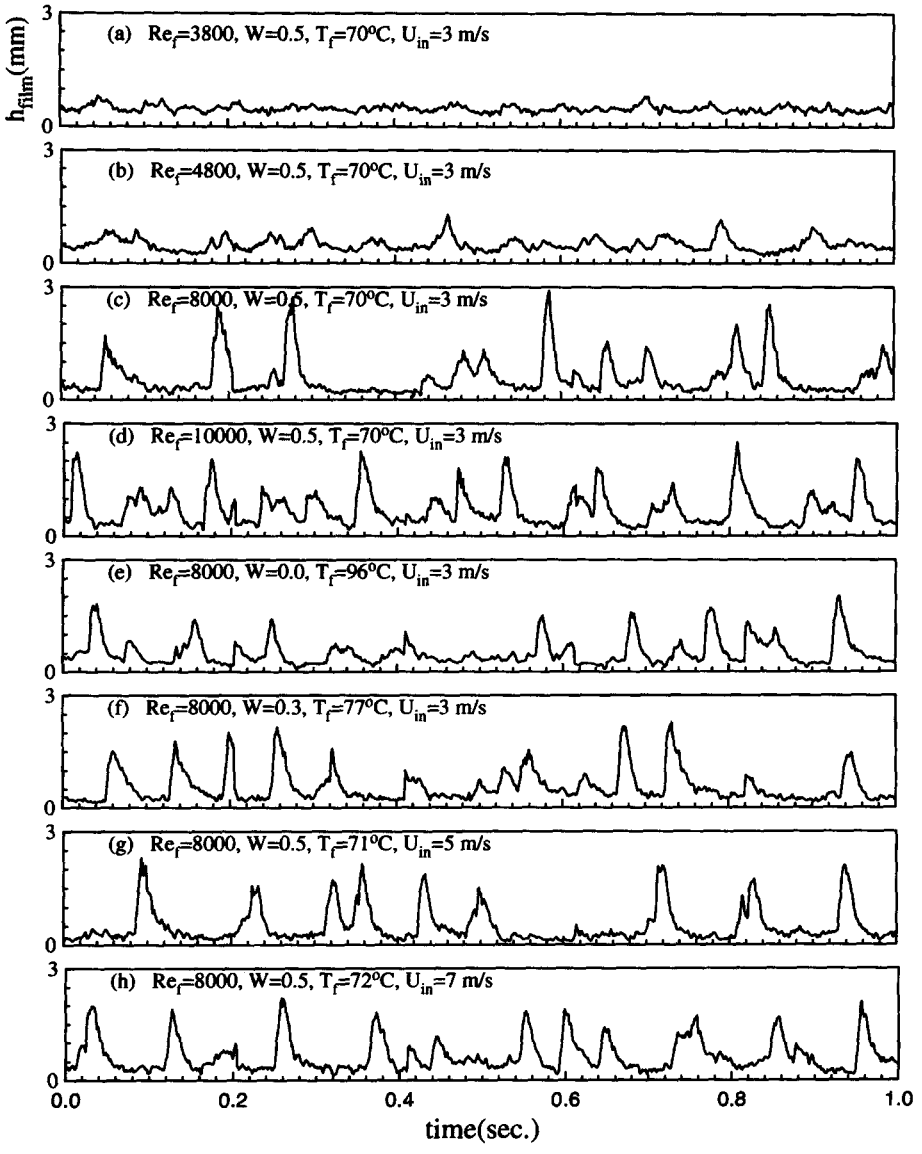

Figure 15. Instantaneous thickness of condensate film.

where $m'(x)$ was mass flow rate per unit depth, and $q(x')$ and i_{fv} were local heat flux and latent heat, respectively. The amount of condensate along the cooling wall can be calculated in the second term of [2]. In this experiment we measured the local heat flux as mentioned in section 2.2, and calculated the film Reynolds number. So, we could investigate the contribution of the second term to the film Reynolds number. For example, in the case of $U_{in} = 7$ m/s, $W = 0.2$, and $Re_{f,in} = 2800$, the second term contributed 6% of the film Reynolds number (Re_f). When vapor velocity (U_{in}) decreased and air–mass fraction (W) increased, the condensing mass flow rate decreased. The contribution was, therefore, less than 6% for the following cases, $U_{in} = 3$, 5, 7 m/s, $W = 0.2$, 0.5, 0.7, and $Re_{f,in} > 2800$.

For the analyses on vapor-side heat transfer coefficient, mixture vapor Reynolds number (Re_v) was defined. The distance from the entrance of the test section, x, was taken for the length scale and the relative velocity of mixture vapor to the interface for the velocity scale. The mixture vapor velocity at $x = 1.3$ m was assumed to equal the inlet velocity of the test section, since the deceleration induced by condensation was low and the acceleration of the mixture vapor in the inviscid core due to the development of boundary layer compensated the deceleration. The

maximum decrease of the bulk mean velocity of mixture vapor due to the condensation was 13.7% of the inlet velocity at $U_m = 3$ m/s and $W = 0.1$. Most cases for mixture vapor condensation in the table 1, the decrement was less than 10%. The vapor Reynolds number (Re_{Dh}) based on the hydraulic diameter of this experiment and the inlet velocity was from 18,000 to 42,000. In this range the velocity in the inviscid core was estimated to increase about 13% at $x = 1.3$ m ($x/D_h = 10.8$) from the Schetz's (1993). The vapor Reynolds number (Re_v) was, therefore, supposed to shift in the range of less than 10%. The interface velocity between condensate and mixture vapor was calculated from the Yih & Liu's turbulence film model (1983). The inlet velocity of the mixture vapor was calculated from the measured mass flow rates of steam and air. All transport properties of mixture vapor were calculated at the arithmetic mean of the bulk and the interface temperature using the mixture property evaluation methods recommended by Reid *et al.* (1988).

3. RESULTS

3.1. Pure steam condensation

Figure 5 shows the local Nusselt number as a function of film Reynolds number (Re_f). Each symbol presents the vapor velocity at the inlet of the test section. The results indicate that the effect of vapor velocity on film-side heat transfer coefficient is negligible in this experimental range. The data of the lowest film Reynolds number at each vapor velocity are the cases without film feeding. The dotted and dashed lines show the results of Chun & Seban's (1971) experimental correlation for evaporation and Nusselt theory (1916) for stagnant vapor condensation respectively.

The solid lines in figure 5 are the best fir of the present data as followings,

$$Nu_w = \frac{h_f(\nu^2/g)^{1/3}}{k} = 0.88Re_f^{-0.25} \quad [3]$$

$$Nu_t = \frac{h_f(\nu^2/g)^{1/3}}{k} = 0.0052Re_f^{0.34}Pr_f^{0.65} \quad [4]$$

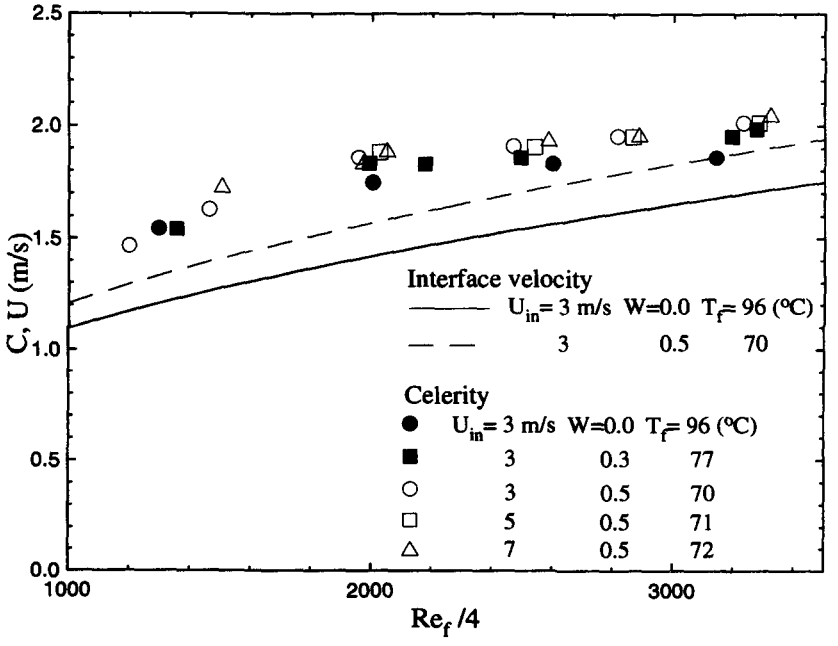

Figure 16. Celerity measured and interface velocity calculated turbulence model (Yih & Liu 1983).

where subscripts, w and t, indicate the flow regime, wavy laminar (pseudo-laminar) and wavy turbulence flow, respectively. Symbols, v and k, are kinematic viscosity and thermal conductivity of condensate film respectively. Also, g is gravitational acceleration. The exponent, -0.25, for wavy laminar flow, is equivalent to the Kutateladze's (1982) analysis which results from slowly moving vapor condensation.

A great number of studies of a pure substance condensation have been conducted experimentally. Most of the published results have shown the mean Nusselt number as a function of Reynolds number and Prandtl number. In order to compare the present data with the previous results, mean Nusselt number was obtained from the integration of local Nusselt number according to the reference (Chun & Seban 1971). The solid and the dashed line in figure 6 are the calculation results from [3] and [4], and Chun & Seban's (1971) correlation at $Pr = 5$ respectively. The symbols scattered widely for turbulent film flow were reconstructed from Kirkbride (1933–1934), and the hatch for wavy film flow came from Kutateladze & Gogonin (1979), who presented the experimental data of slowly moving vapor condensation on vertical tubes.

3.2. Steam–air condensation

Overall heat transfer coefficient. The most important difference of condensation between pure steam and mixture vapor with a noncondensable gas is the existence of additional thermal resistance in the mixture vapor. The resistance is due to the boundary layer of a noncondensable gas adjacent to the condensate film through which steam must diffuse to the interface.

Figure 7 shows heat transfer coefficient along the condensing surface, when the extra condensate is not fed. The open circles result from Huhtiniemi & Corradini's (1993) data obtained at a vertical wall. The air–mass fractions of the present result and Huhtiniemi & Corradini's (1993) are 0.7 and 0.78, respectively. The temperatures of condensing wall are 31.2 and 29.7°C, respectively.

Figures 8–10 show an overall heat transfer coefficient as a function of Re_f in various air–mass fractions and mixture vapor velocities. In the figures, U_{in} and U_m are the bulk mean velocity at the inlet of the test section and the interval where h_o is obtained. The decrease of the bulk mean velocity is caused by condensing mass flux. At some instance ($W = 0.2$, $U_{in} = 7$ m/s; $W = 0.3$, $U_{in} = 7$ m/s) the overall heat transfer coefficients decrease clearly up to a certain Re_f and increase again with the increase of Re_f as in falling-film condensation of pure steam. In other instance the overall heat transfer coefficients increase monotonously with the increase of Re_f. This is because the overall heat transfer coefficients depend on the thermal resistance in the both side of film and mixture vapor. The decrease is expected when the thermal resistance of vapor-side is comparable to and inferior to that of film-side for low air–mass fraction and high mixture vapor velocity.

From the present results of a pure steam condensation, it is expected that film-side thermal resistance increases up to a transition Re_f, for a wavy laminar film flow, and decreases with the increase of Re_f over the transition, for a turbulent film flow. On the other hand, the thermal resistance of vapor-side might have two counteractive effects with the increase of Re_f. The rough and dynamic surface of condensate film is supposed to enhance the mixing of steam–air flow in the diffusion layer, while the decrease of the relative velocity of the mixture vapor to the condensate film is expected to suppress the convective transport.

Vapor-side heat transfer coefficient. If a difference of interface structure with a different gas phase (pure steam and steam–air mixture) is not great to change heat transfer mechanism in the film, the film-side heat transfer coefficient can be estimated from the results of a pure steam condensation. Since the effect of surface waves on the transport of heat and mass in the diffusion layer was essential issue in this work, the vapor-side heat transfer coefficient was reduced from the overall and the film-side heat transfer coefficient.

The key is how to estimate the interface temperature between the mixture vapor and the condensate film. No technique is available for the direct measurement of the interface temperature with sufficient accuracy because of the interface movement. So, the interface temperature has to be reasonably estimated from an indirect method. We estimated the interface temperature in the following equation:

$$T_i = \frac{q(x)}{h_f} + T_w \qquad [5]$$

where $q(x)$ and T_w were the heat flux and the wall temperature measured. Equations [3] and [4] obtained in the pure steam condensation were used for the film-side heat transfer coefficient (h_f) of mixture vapor condensation.

This is based on the assumption that the film-side thermal resistance depends on the fluid properties and flow characteristics of only the condensate film regardless of components of vapor, for example, pure steam or steam–air mixture. On considering that Nusselt number is well correlated as a function of Re_f and Pr_f except the high interfacial shear stress, we can easily accept the assumption. There is an argument that surface tension and condensing mass flux affect the wave structure of condensate film. In this experimental range such as high film Reynolds number and moderate mixture vapor velocity, however, it is expected that the effect of surface tension and condensing mass flux on film-side heat transfer is negligible as compared with that of Re_f and Pr_f. It has been argued that small wave amplitude highly depends on the interfacial conditions such as surface tension and condensing mass flux, but that large wave amplitude is stolid to the interfacial conditions. The flow characteristics for a vertical free falling-film is affected largely by large waves than small waves. It is, therefore, reasonable that the non-dimensional film-side heat transfer coefficient, $(h_f(v^2/g)^{1/3})/k$, is considered as only Re_f and Pr_f in this experimental range. If the non-dimensional film-side heat transfer coefficient is accepted as a function of only Re_f and Pr_f, the assumption that [3] and [4] can be applied to the film-side heat transfer coefficient of steam–air condensation is reasonable.

Figures 11–13 show the vapor-side heat transfer coefficients, which is estimated from the overall heat transfer coefficients in figures 8–10. The horizontal axes are the Reynolds number of mixture vapor flow based on the relative velocity of mixture vapor to the interface velocity. The arrows indicate the increase of Re_f. Since the velocity of condensate film was not negligible for high film Reynolds number, the effect of surface waves on the diffusion layer was considered at the relative velocity. So, Re_v decreases as Re_f increases. The solid lines in the figures indicate the heat transfer coefficient calculated from the Colburn and Chilton–Colburn analogy for a smooth flat plate (Kim & Corradini 1990). They are the heat transfer coefficient of which the mixture vapor with the same relative velocity condenses on a smooth flat plate. That is, the differences between the symbols and the line are the enhancement of vapor-side heat transfer coefficient due to surface waves. The absolute increment of the vapor-side heat transfer coefficient is greater for low air–mass fraction, $W = 0.2$, than for high air–mass fraction, $W = 0.5$. Also, the enhancement effect is greater for low mixture vapor velocity, $U_m = 3$ m/s, than for high mixture vapor velocity, $U_{in} = 7$ m/s.

The ratio of the present experimental results (symbols in figures 11–13) to the estimated values by the analogy for a flat plate (solid line in figures 11–13) is shown in figure 14 for various surface waves present with Re_f. All the experimental data listed in table 1 are presented. That is the enhancement effect of vapor-side heat transfer due to the surface waves of condensate film. The horizontal axis is Re_v, and the symbols show the bandwidth of Re_f. The comparison shows clearly that the effect of surface waves on the heat transfer enhancement can be expressed as non-dimensional number Re_f and Re_v in this experimental range. The enhancement effect increases with the increase of Re_f and decreases with the increase of Re_v.

3.3. *Instantaneous thickness of condensate film*

Figure 15 shows the instantaneous thickness of condensate film at various vapor velocities, air–mass fractions, and condensate film Reynolds numbers. Film thickness with film Reynolds numbers at the same air–mass fraction ($W = 0.5$) and film temperature ($T_f = 70°C$) is presented in figure 15 (a)–(d). Figure 15 (e), (f) and (c) are film thickness with air–mass fractions at the same film Reynolds number ($Re_f = 8000$) and mixture vapor velocity ($U_{in} = 3$ m/s). Also, figure 15 (c), (g) and (h) is film thickness with mixture vapor velocities at the same film Reynolds number ($Re_f = 8000$) and air–mass fraction ($W = 0.5$). All cases were measured at 1.3 m downstream from the inlet. The film temperature is the average of the inlet and the outlet as described in figure 1.

As film Reynolds number increases, a large amplitude waves appear frequently. It has been known that large amplitude waves are related to the dynamics of condensate film flow, and that small amplitude waves found on the substrate and the large amplitude waves are related to the

transport of heat and mass in the gas flow. It is expected that the dynamic motion of surface waves such as propagation enhances heat and mass transfer in the film and the mixture vapor layer.

Wave celerity (C) was calculated from the cross-correlation of the instantaneous film height simultaneously measured at two locations. Figure 16 shows the celerity measured in this experiment and the interface velocity (U) calculated from Yih & Liu's (1983) turbulence film model. Each symbol shows the celerity in various conditions. The solid and dashed lines indicate the interface velocity in different film temperatures. The celerity and the interface velocity show that the velocity of condensate film is not negligible as compared with the mixture vapor velocity in the present experimental range. So, vapor-side heat transfer coefficients were analyzed at the relative coordinate on the moving film.

4. CONCLUDING REMARKS

For a pure steam condensation, local Nusselt number was obtained in a broad range of film Reynolds number and correlated as a function of film Reynolds number and Prandtl number. For a steam–air condensation, overall heat transfer coefficient decreased with the increase of air–mass fraction, and increased with the increase of mixture vapor velocity. In a given air–mass fraction and mixture vapor velocity, overall heat transfer coefficient has two trend as film Reynolds number increases. If the vapor-side thermal resistance is dominant as compared with the overall resistance, the overall heat transfer coefficient monotonously increases because of a dynamic motion of the surface waves on condensate film. If the thermal resistance of film-side and vapor-side is comparable, however, the overall heat transfer coefficient decreases for low film Reynolds number like the pure steam condensation.

The comparison showed clearly that the vapor-side heat transfer coefficient increased with the increase of condensate film Reynolds number. The enhancement effect of vapor-side heat transfer coefficient induced by a dynamic interaction of the surface waves and the diffusion layer depends on film Reynolds number and mixture vapor Reynolds number. The enhancement effect is high for low mixture vapor Reynolds number and decreases with the increase of mixture vapor Reynolds number.

Also, the instantaneous thickness of condensate film and the wave celerity were presented in various air–mass fractions, mixture vapor velocities and condensate film Reynolds numbers. The wave amplitude and the wave celerity increased with the increase of film Reynolds number are supposed to enhance the transport of heat and mass in the diffusion layer.

Acknowledgements—This work was performed with the support of KAERI (Korea Atomic Energy Research Institute) and AFERC (Advanced Fluid Engineering Research Center). The authors are grateful for these supports.

REFERENCES

Al-Diwany, H. K. & Rose, J. W. 1973 Free convection film condensation of steam in the presence of non-condensing gases. *Int. J. Heat Mass Transfer* **16,** 1359–1369.

Asano, K. & Nakano, Y. 1979 Forced convection film condensation of vapors in the presence of noncondensable gas on a small vertical flat plate. *J. Chem. Engr. of Japan* **12,** 196–202.

Bean, H. S. 1971 *Fluid Meters—Their Theory and Application.*

Chang, H.-C. 1994 Wave evolution on a falling film. *Ann. Rev. Fluid Mech.* **26,** 103–136.

Chu, K. J. & Dukler, A. E. 1974 Statistical characteristics of thin, wavy films: Part II. Studies of the substrate and its wave structure. *AIChE J.* **20,** 695–706.

Chu, K. J. & Dukler, A. E. 1974 Statistical characteristics of thin, wavy films: Part III. Structure of the large waves and their resistance to gas flow. *AIChE J.* **21,** 583–593.

Chun, K. R. & Seban, R. A. 1971 Heat transfer to evaporating liquid films. *J. Heat Transfer* **93,** 391–396.

Dallmeyer, H. 1970 Stoff-und Warmeubertragung bei der Kondensation eines Dampfes aus einem Gemisch mit einem nicht kondensierenden Gas in Laminarer und turbulenter Stromungsgrenzschicht. *VDL-Forschungsheft* **539,** 5–24.

Denny, V. E. & Jusionis, V. J. 1972 Effect of noncondensable gas and forced flow on laminar film condensation. *Int. J. Heat Mass Transfer* **15,** 315–326.

Denny, V. E., Mills, A. F. & Jusionis, V. J. 1971 Laminar film condensation from a steam–air mixture undergoing forced flow down a vertical surface. *Trans. ASME* **93,** 297–304.

Henderson, C. L. & Marchello, J. M. 1969 Film condensation on the presence of a condensable gas. *J. Heat Transfer* **91,** 447–450.

Huhtiniemi, I. K. & Corradini, M. L. 1993 Condensation in the presence of noncondensable gases. *Nucl. Engrg Des.* **141,** 429–446.

Kang, H. C. & Kim, M. H. 1992 Measurement of three-dimensional wave form and interfacial area in an air–water stratified flow. *Nucl. Engrg Des.* **136,** 347–360.

Kang, H. C. & Kim, M. H. 1992 The development of a flush-wire probe and calibration method for measuring liquid film thickness. *Int. J. Multiphase Flow* **18,** 423–437.

Kang, H. C. & Kim, M. H. 1994 Effect of non-condensable gas and wavy interface on the condensation heat transfer in a nearly horizontal plate. *Nucl. Engrg Des.* **149,** 313–321.

Karapantsios, T. D., Kostoglou, M. & Karabelas, A. J. 1995 Local condensation rates of steam–air mixtures in direct contact with a falling liquid film. *Int. J. Heat Mass Transfer* **38,** 779–794.

Karapantsios, T. D. & Karabelas, A. J. 1995 Direct-contact condensation in the presence of noncondensables over free-falling films with intermittent liquid feed. *Int. J. Heat Mass Transfer* **38,** 795–805.

Kellenbenz, J. & Hahane, E. 1994 Condensation of pure vapours and binary vapour mixtures in forced flow. *Int. J. Heat Mass Transfer* **37,** 1269–1276.

Kim, M. H. & Corradini, M. L. 1990 Modeling of condensation heat transfer in a reactor containment. *Nucl. Engng Des.* **118,** 193–212.

Kirkbride, C. G. 1933–1934. Heat transfer by considering vapor on vertical tubes. *Trans. AIChE* **30,** 170–185.

Kutateladze, S. S. & Gogonin, I. I. 1979 Heat transfer in film condensation of slowly moving vapour. *Int. J. Heat Mass Transfer* **22,** 1593–1598.

Kutateladze, S. S. 1982 Semi-empirical theory of film condensation of pure vapours. *Int. J. Heat Mass Transfer* **25,** 653–660.

Legay-Desesquelles, F. & Prunet-Foch, B. 1986 Heat and mass transfer with condensation in laminar and turbulent boundary layers along a flat plate. *J. Heat Mass Transfer* **29,** 95–105.

Minkowycz, W. J. & Sparrow, E. M. 1966 Condensation heat transfer in the presence of noncondensables, interfacial resistance, superheating, variables properties, and diffusion. *Int. J. Heat Mass Transfer* **9,** 1125–1144.

Nusselt, W. 1916 Die Oberflachenkondensation de Wasserdampfes. *Zieschrift Ver. Deut. Ing.* **60,** 541.

Othmer, D. 1929 The condensation of steam. *Industrial and Engineering Chemistry* **21,** 577–583.

Peterson, P. F., Schrock, V. E. & Kageyama, T. 1993 Diffusion layer theory for turbulent vapor condensation with noncondensable gases. *Trans. ASME* **115,** 998–1003.

Reid, R. C., Prausnitz, J. M. & Poling, B. E. 1988 *The Properties of Gases and Liquids.* McGraw-Hill, New York.

Schetz, J. A. 1993 *Boundary Layer Analysis.* Prentice-Hall, New Jersey.

Sparrow, E. M., Minkowycz, W. J. & Saddy, M. 1967 Forced convection condensation in the presence of noncondensables and interfacial resistance. *Int. J. Heat Mass Transfer* **10,** 1829–1844.

Sleger, L. & Seban, R. A. 1970 Laminar film condensation of steam containing small concentration of air. *Int. J. Heat and Mass Transfer* **13,** 1941–1947.

Spindler, B. 1982 Linear stability of liquid films with interfacial phase change. *Int. J. Heat Mass Transfer* **25,** 161–173.

Yih, S. & Liu, J. 1983 Prediction of heat transfer in turbulent falling liquid film with or without interfacial shear. *AIChE J.* **29,** 903–909.